



Receiver bias estimation and validation of e-POP GAP-O ionospheric radio occultation measurements

C. Watson^{*(1,2)}, R.B. Langley⁽³⁾, D.R. Themens⁽⁴⁾, A.W. Yau⁽²⁾, A. Howarth⁽²⁾, and P.T. Jayachandran⁽⁴⁾

(1) University Corporation for Atmospheric Research, COSMIC Program Office, Boulder, CO, USA

(2) University of Calgary, Department of Physics and Astronomy, Calgary, AB, Canada

(3) University of New Brunswick, Department of Geodesy and Geomatics Engineering, Fredericton, NB, Canada

(4) University of New Brunswick, Physics Department, Fredericton, NB, Canada

Abstract

This paper presents validation of ionospheric Global Positioning System (GPS) radio occultation (RO) measurements of the GPS Attitude, Positioning, and Profiling Experiment occultation receiver (GAP-O). The primary source of uncertainty impacting GAP-O data products is the receiver differential code bias (rDCB). A minimization of standard deviations (MSD) technique for rDCB estimate has shown the most promise, and resulted in estimates ranging from -39 to -29 TECU, including a steady, long term decrease in rDCB magnitude. MSD estimates agree well with the “assumption of zero topside TEC” method at satellite apogee in the polar cap.

Bias-corrected topside TEC of GAP-O was validated by statistical comparison with topside TEC obtained from ground-based GPS TEC and ionosonde measurements. GAP-O and ground-based topside TEC had similar variability, however GAP-O consistently underestimated the ground-derived topside TEC by up to 8 TECU. Ionospheric electron density profiles obtained from Abel inversion of GAP-O occultation TEC showed consistently good agreement with F-region densities of incoherent scatter radar measurements, however RO-derived E-region densities were not as reliable at high latitudes.

1. Introduction

The GAP instrument [1] is one of eight components of the Enhanced Polar Outflow Probe (e-POP) instrument suite onboard the Cascade Smallsat and Ionospheric Polar Explorer (CASSIOPE) satellite launched on September 29, 2013. e-POP was designed to study solar wind-magnetosphere-ionosphere coupling processes and ionospheric dynamics in the polar regions [2]. CASSIOPE was launched into an elliptical low Earth orbit (LEO) with a perigee of 325 km, apogee of 1490 km, and inclination of 81°. Orbit apogee has decreased to ~1325 km as of November 2016. The high inclination, elliptical orbit of CASSIOPE, combined with the high-data-rate GAP-O receiver, provides unique RO and topside observations of the high latitude ionosphere, including the characteristics of small scale plasma irregularities in the polar and auroral regions [3].

There are several well-established methods for satellite and receiver bias estimation using ground-based receiver networks [4], which, for LEO purposes, provide reliable GPS satellite bias estimates, but are unsuitable for receiver bias determination due to the fast moving satellite, variable satellite altitude, and high multipath LEO environment. For the FORMOSAT-3/COSMIC mission, a previous report [5] found that the “zero-TEC method” produced an rDCB estimate with an uncertainty range of +/- 2.9 TECU, which was influenced by multipath and phase-levelling errors. Estimation of GAP-O receiver bias presents a unique challenge due to the highly elliptical CASSIOPE orbit and intermittent availability of GAP-O measurements (typically 0.5-3 hours per day).

The objective of this paper is to provide a reliable estimate of GAP-O receiver bias, and to assess the accuracy and reliability of GAP-O topside TEC and RO density profile data products. GAP-O topside TEC was compared with topside TEC computed from ground-based ionosonde and GPS TEC measurements of the Canadian High Arctic Ionospheric Network (CHAIN) [6], for intervals where CASSIOPE was located above a ground station and near the F-region density peak (hmF2). Resolute (74.75°N, 265.00°E) incoherent scatter radar (ISR) measurements were used in place of ionosonde measurements, when available. GAP-O electron density profiles derived from inversion of RO TEC were validated using measurements of the Millstone Hill (42.62° N, 288.51°E) and Poker Flat (65.13°N, 212.53°E) ISRs, located at mid and auroral latitudes, respectively.

2. GAP-O Measurements

GAP-O uses a NovAtel OEM4-G2L dual-frequency GPS receiver for tracking GPS broadcasts at L1 (1575.42 MHz) and L2 (1227.60 MHz) frequencies, which is fed by an anti-ram facing modified NovAtel GPS-702 pinwheel antenna. GAP-O records L1 and L2 pseudorange and carrier-phase observables at a rate of 20 Hz, 50 Hz, or 100 Hz, depending on experiment requests. Code and phase-derived TEC were computed from the relative delays of received pseudorange and carrier signals. GPS satellite DCBs were obtained from the Center for Orbit

Determination (CODE) database of the University of Bern (<ftp://ftp.unibe.ch/aiub/CODE/>).

On active days, the GAP-O receiver typically records between 0.5 and 3 hours of data. Intervals of data availability are based on e-POP experiment requests submitted to the University of Calgary e-POP science team, with the bulk of measurement requests at northern high latitudes and over Canada. For 1 Oct. 2013 to 1 Nov. 2016, there were a total of 1971 experiments run, with 8142 occultation events containing useable data. Figure 1 shows a map of occultation tangent points at peak F region density (NmF2) for the first 37 months of GAP-O operation. The high occurrence of occultations in auroral and polar regions is evident.

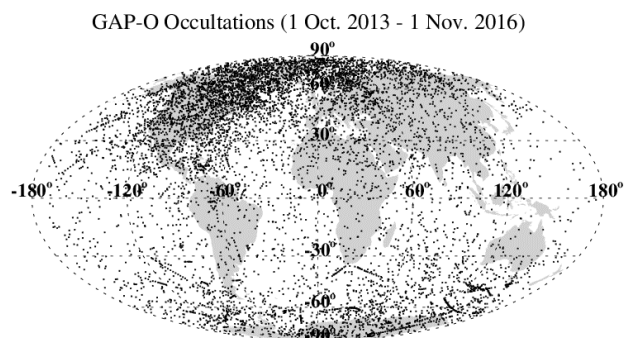


Figure 1. Coordinates of GAP-O occultation tangent points at NmF2 for 1 Oct. 2013 to 1 Nov. 2016.

3. Receiver DCB Estimate

3.1 Minimization of Standard Deviations

The minimization of standard deviations (MSD) technique for rDCB estimation has been applied to ground-based rDCB estimation at high latitudes [7]. In a nutshell, the MSD method involves comparing vertical TEC ($vTEC$) calculated from multiple GPS satellites, while testing a range of bias values to determine the receiver bias that results in the closest correspondence between $vTECs$. The “test” bias that results in the best agreement between $vTECs$ (i.e. the minimum standard deviation of $vTECs$ over the experiment time interval), is taken as the rDCB estimate for that experiment. A satellite elevation angle cutoff of 20° was applied in all calculations. Vertical TEC was calculated by applying a mapping function that projects slant TEC to the vertical. Four mapping functions were tested: the “thin layer model” (TLM), the “F&K” projection, the “Lear” projection, and a “sine” projection. Mapping functions have been examined in detail in previous studies [8].

For 1 Oct. 2013 to 1 Nov. 2016, Figure 2 plots (a) daily GAP-O rDCB estimates from the MSD method and four mapping functions, (b) a ten-day running average and standard deviation of daily estimates, (c) the daily root mean square (RMS) of pseudorange multipath combinations MP_1 and MP_2 [5] at L1 and L2 frequencies,

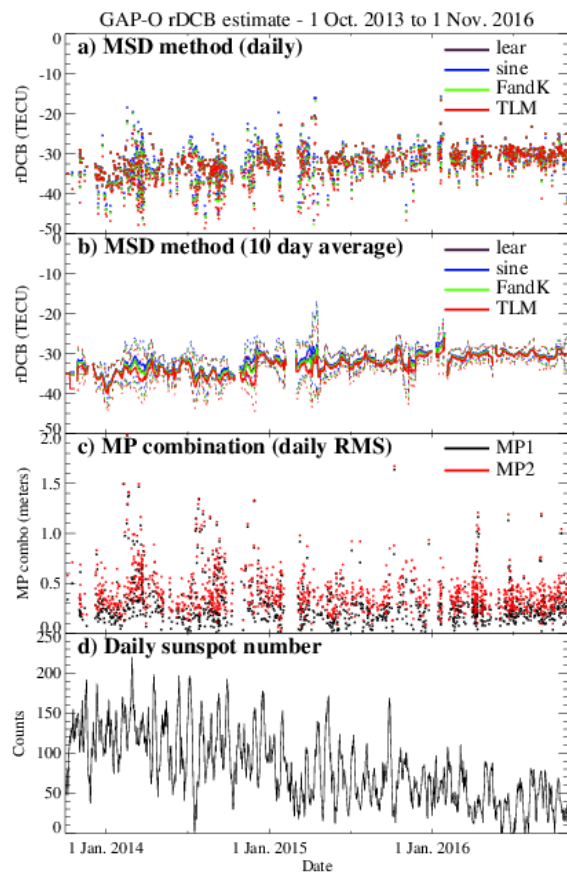


Figure 2. (a) Daily rDCB estimates, (b) ten-day running average (solid lines) and \pm the standard deviation (dashed lines) of rDCB estimates, (c) daily RMS L1 and L2 multipath combinations, and (d) daily sunspot number.

and (d) the daily sunspot number. Significant day-to-day variability in the rDCB estimate is evident until early 2015, with intervals of highest daily rDCB variability corresponding to intervals of highest $MP_{1,2}$. Beginning in March-April 2015, daily rDCB estimates stabilize, showing significantly less day-to-day variability. The occurrence of high $MP_{1,2}$ values also decreases in early 2015, which may improve the phase levelling accuracy and thus result in more consistently accurate rDCB estimates. A significant decrease in solar activity into 2016 may also contribute to the increased rDCB stability, since the occurrence of ionization structures in the polar cap ionosphere is known to decrease with solar activity [9]. A long-term decrease in average rDCB magnitude from ~ 35 TECU to ~ 30 TECU is also evident.

3.2 “Zero TEC” Method

Figure 3 shows biased slant TEC above CASSIOPE for (a) north and (b) south polar cap passes ($>70^\circ$ and $<-70^\circ$ magnetic latitude), where average slant TEC from all satellites above 20° elevation angle was recorded at maximum CASSIOPE altitude for each pass. CASSIOPE altitude is color coded, with red indicating TEC recorded near satellite apogee. As expected, there was significantly more electron content above CASSIOPE at lower

altitudes, particularly in 2013 and early 2014. For altitudes of 1200-1500 km, biased TEC above CASSIOPE was consistently around -37 to -30 TECU, with the standard deviation of each red cluster of data points ranging from 1.0 to 2.5 TECU. Assuming negligible TEC above CASSIOPE near apogee, this indicates good agreement between rDCB estimates of the “Zero TEC” and MSD methods. Linear fits of biased topside TEC near apogee (red dashed line) and MSD rDCB estimates (grey dashed line) in Figure 3 also show very similar long term trends.

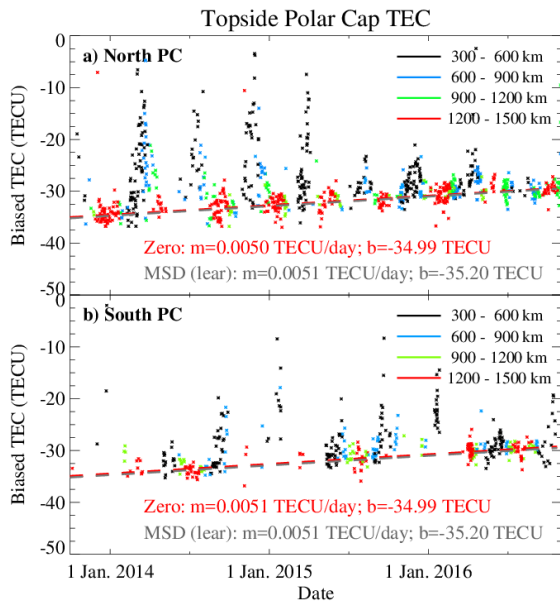


Figure 3. Biased topside average slant TEC above CASSIOPE for (a) north and (b) south polar cap (PC) passes, color coded based on CASSIOPE altitude. Dashed lines show linear fits of biased TEC near satellite apogee (red) and rDCB estimates of the MSD method with a “Lear” projection (grey), with slope (m) and y-intercept (b) of linear fits listed in each panel.

4. Data Validation

4.1 Topside TEC

Absolute topside TEC of GAP-O was compared to topside TEC calculated from measurements of co-located ground Canadian Advanced Digital Ionosondes (CADIs) and GPS receivers of CHAIN. For CASSIOPE passes above a ground station (within 300 km) at an altitude close to hmF2, topside TEC above CASSIOPE was calculated by taking the vertical TEC of the ground receiver and subtracting the height integrated bottomside electron density of CADI. CADI profiles were extrapolated to CASSIOPE altitude using an alpha-Chapman function when needed (no more than 50 km above hmF2). Figure 4 shows GAP-O topside TEC and ground-derived topside TEC for CASSIOPE passes over 5 different ground stations in the northern polar cap. Error bars indicate RMS deviations for these calculations. For Resolute, the first three events (indicated by large dots)

used Resolute ISR (RISR) measurements in place of CADI. Trends in GAP-O and ground-derived topside TEC agree reasonably well, however, GAP-O almost always underestimated the topside TEC compared to ground measurements by up to 8 TECU. Possible explanations for this systematic offset include differences arising from the projection of slant TEC to vertical on the ground compared to the vertical projection at LEO, a systematic error in the GAP-O rDCB estimate, or errors in the extrapolation of CADI profiles above NmF2.

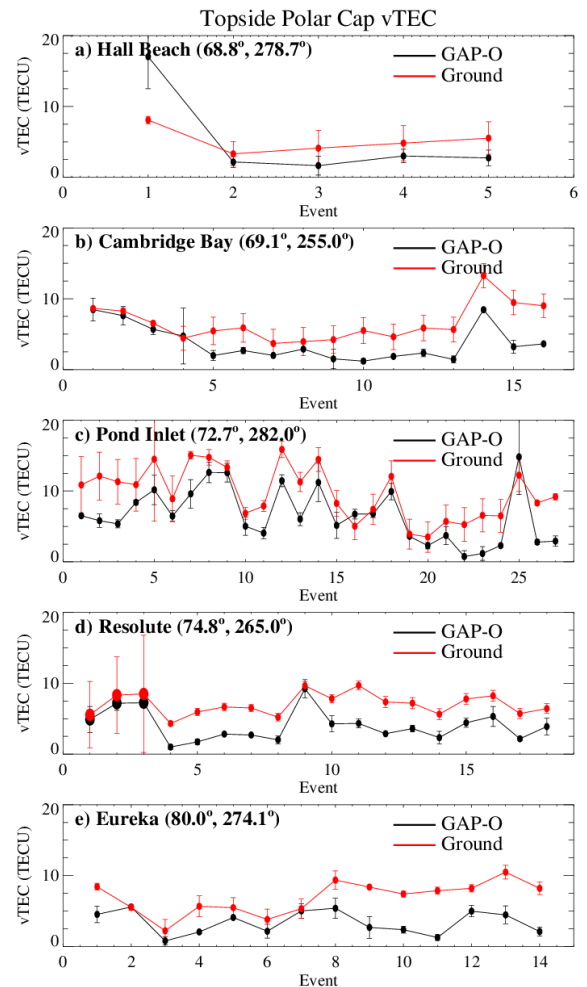


Figure 4. Topside polar cap vertical TEC calculated from GAP-O measurements (black) and from ground GPS TEC and ionosonde (small dot)/RISR (large dot) measurements (red). Geodetic coordinates of ground stations are shown in each panel.

4.2 Ionosphere Density Profiles

To calculate ionospheric electron density profiles from GAP-O measurements, unbiased TEC during RO events was subjected to an Abel inversion, following [10]. Figure 5 shows sample GAP-O electron density profiles (red) and ISR measurements (black/grey dots) from occultations near the field of view of the (a) Millstone Hill Steerable Antenna (MISA) and the (b) Poker Flat ISR (PFISR), where red dashed lines represent the uncertainty in GAP-O profiles based on the standard deviation of

estimated GAP-O rDCB in Figure 2b. Coordinated Universal Time and geodetic coordinates of the occultation tangent point at NmF2 are indicated in each panel, along with NmF2 and hmF2 from ISR and GAP-O measurements. ISR measurements for both long pulse (LP) and alternating code (AC) modes are shown, with horizontal lines indicating the standard deviation of measurements for the duration of the occultation event. GAP-O and ISR density profiles show good agreement in the F region, while E region profiles in Figure 5a also closely match. E region densities typically show less agreement at high latitudes (Figure 5b), which may be in part due to the highly structured polar and auroral ionospheres.

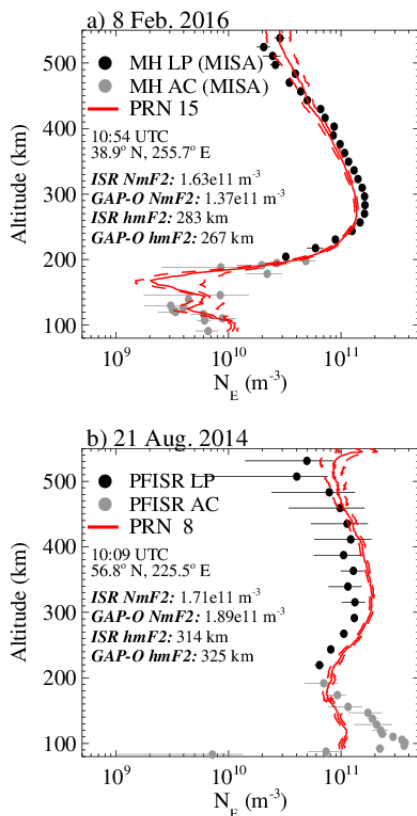


Figure 5. GAP-O electron density profiles (red) and ISR measurements of (a) Millstone Hill and (b) Poker Flat. UTC and geodetic coordinates of the occultation tangent point at hmF2, along with NmF2 and hmF2 of ISR and GAP-O profiles, are listed in each panel.

5. Acknowledgements

CADI and ground GPS data is from the Canadian High Arctic Ionospheric Network (CHAIN) of the University of New Brunswick (UNB) Physics Department (<http://chain.physics.unb.ca/chain/>). Millstone Hill, Resolute, and Poker Flat Incoherent Scatter Radar data was obtained from the Madrigal Database (<http://madrigal.haystack.mit.edu/madrigal/index.html>), with the kind permission of Phil Erickson and Roger Varney. Daily sunspot number data is from WDC-SILSO, Royal Observatory of Belgium, Brussels (<http://www.sidc.be/silso/datafiles>). Richard B. Langley

and Andrew W. Yau acknowledge funding support from the Natural Sciences and Engineering Research Council of Canada and the Canadian Space Agency.

6. References

1. D. Kim and R.B. Langley, "The GPS Attitude, Positioning, and Profiling Experiment for the Enhanced Polar Outflow Probe Platform on the Canadian CASSIOPE satellite," *Geomatica*, **64**, 2, 2010, 233-243.
2. A.W. Yau and H.G. James, "CASSIOPE Enhanced Polar Outflow Probe (e-POP) mission overview," *Space Sci. Rev.*, **189**, 2015, 3-14, doi:10.1007/s11214-015-0135-1.
3. E.B. Shume, A. Komjathy, R.B. Langley, O. Verkhoglyadova, M.D. Butala, and A.J. Mannucci, "Intermediate scale plasma irregularities in the polar ionosphere inferred from GPS radio occultation," *Geophys. Res. Lett.*, **42**, 3, 2015, 688-696, doi:10.1002/2014GL062558.
4. A. Komjathy, L. Sparks, B.D. Wilson, and A.J. Mannucci, "Automated daily processing of more than 1000 ground-based GPS receivers for studying intense ionospheric storms," *Radio Sci.*, **40**, RS6006, 2005, doi:10.1029/2005RS003279.
5. P. Stephens, A. Komjathy, B. Wilson, and A. Mannucci, "New leveling and bias estimation algorithms for processing COSMIC/FORMOSAT-3 data for slant total electron content," *Radio Science*, **46**, RS0D10, 2011, doi:10.1029/2010RS004588.
6. P.T. Jayachandran, R.B. Langley, J.W. MacDougall et al., "Canadian High Arctic Ionospheric Network (CHAIN)," *Radio Sci.*, **44**, RS0A03, 2009 doi:10.1029/2008RS004046.
7. D.R. Themens, P.T. Jayachandran, R.B. Langley, J.W. MacDougall, and M.J. Nicolls, "Determining receiver biases in GPS-derived total electron content in the auroral oval and polar cap region using ionosonde measurements," *GPS Solut.*, **17**, 2012, 357-369, doi:10.1007/s10291-012-0284-6.
8. J. Zhong, L. Jiuhou, X. Dou, and Y. Xinan, "Assessment of vertical TEC mapping functions for space-based GNSS observations," *GPS Solut.*, **20**, 2016, 353-362, doi:10.1007/s10291-015-0444-6.
9. C. Watson, P.T. Jayachandran, and J.W. MacDougall, "Characteristics of GPS TEC variations in the polar cap ionosphere," *J. Geophys. Res. Space Physics*, **121**, 2016, 4748-4768, doi:10.1002/2015JA022275.
10. W.S. Schreiner, S.V. Sokolovskiy, C. Rocken, and D.C. Hunt, "Analysis and validation of GPS/MET radio occultation data in the ionosphere," *Radio Sci.*, **34**, 4, 1999, 949-966, doi:10.1029/1999RS900034.